

Observing STDP of pyramidal cell and attached interneuron microcircuit using detailed Ca^{2+} dynamics

Lynsey A. McCabe, Bernd Porr, Paolo Di Prodi, Florentin Wörgötter

Department of Electronics and Electrical Engineering

University of Glasgow

United Kingdom, G12 8QQ

e-mail: lmc@elec.gla.ac.uk.

May 6, 2008

Abstract

Synaptic plasticity changes reactive to the timing of pre- and postsynaptic activity is collectively known as spike-timing-dependent plasticity, or STDP. We present a model where LTD is described using the leaky integrator filtering of the change in Ca^{2+} concentration. The model consists of a pyramidal cell, attached interneuron performing feedback inhibition and detailed Ca^{2+} dynamics. We show that attaching an interneuron to the pyramidal cell will greatly alter the overall asymmetry of the STDP curve, particularly observing a distinct reduction in LTD magnitude. By reducing the NMDA-R activity, there is an overall reduction in the magnitude of the weight-change curve along with a distinct alteration to the STDP curve shape. It is seen in our model that the greater the inhibition to the pyramidal cell, the *less* LTD is seen.

1 Introduction

Synaptic weight-change sensitive to the relative timing of pre- and postsynaptic activity is better identified as STDP (spike-timing-dependent plasticity) [1, 2, 3]. This phenomenon can be split into two parts known as LTP and LTD. LTP, or “long-term potentiation”, is the continued elevation of synaptic strength between two neurons during transient neuronal activity. It usually occurs when the presynapse of a neuron is stimulated milliseconds before the postsynaptic neuron.

When the coincidence-timing of stimulation is reversed and the postsynaptic neuron is stimulated before the presynaptic neuron, LTD or “long-term depression” is observed. LTD can be partly explained by this reversal in stimulation timing, which causes a noticeable decline in synaptic strength. Both of these changes in synaptic plasticity are collectively known as spike-timing-dependent plasticity (STDP).

Before the term long-term potentiation was conceived, a hypothesis by Donald Hebb in 1949 [4] was the first step towards understanding how repeated stimulation of two neurons can cause an increase in plasticity. This hypothesis is now known as “Hebbian learning” and states that learning should occur when two neurons repeatedly fire together due to a strengthening in plasticity between them. Unlike Hebbian learning, LTP depends on the specific order that neurons spike to ensure a potentiation in synapse strength. This was seen in 1997-1998 by Markram, Magee, and followed shortly by Bi and Poo [1, 2, 3]. These groups, amongst others, looked specifically at the coincidence timing of stimulation of a pre- and postsynaptic neuron and showed that the timing of action potentials between them was essential in the directionality of plasticity.

It is still a popular area of research because unlike LTP, there is still much hypothesising about which mechanisms are responsible for LTD.

We will show how STDP can be modelled using a calcium dynamics hypothesis by Aihara [5], along with a suggested relationship between Ca^{2+} dynamics and long term depression by Tanaka [6]. We will look at the difference between our new detailed learning rule compared to differential hebbian learning rules such as ISO learning[7, 8, 9, 10], which do not include biophysical realism in their models.

Ca^{2+} dynamics will also be discussed and it is shown using our biologically realistic learning rule that it is possible to emulate results seen in vitro [1, 2, 3]. By using a leaky integrator model of

LTD in conjunction with detailed Ca^{2+} dynamics, we have been able to use a single learning rule that is capable of modelling both LTD and LTP during STDP simulations.

2 The Model

The model was created using a custom-compiled version of the GENESIS-sim 2.3 modelling tool (<http://www.GENESIS-sim.org/GENESIS>) and consists of a cortical pyramidal cell and attached GABAergic inhibitory interneuron (Fig. 1).

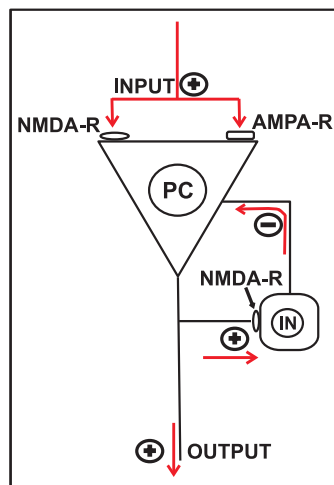


Figure 1: Graphical representation of model designed using the GENESIS-sim software. Here we can see the excitatory “input” which is the modelled presynaptic input into the pyramidal cell. The modelled action potential is simply a delta impulse function, $\delta(t)$. Attached to the pyramidal cell are AMPA and NMDA receptors. A current injection into the pyramidal cell stimulates the neuron enough to generate the postsynaptic action potential. This travels from the pyramidal cell body and the axon activating the NMDA receptors on the GABAergic interneuron, allowing an influx of Ca^{2+} into the cell. If the excitation is strong enough the interneuron releases GABAergic neurotransmitters back to the pyramidal cell, inhibiting as it does so. Both the pyramidal cell and interneuron use the Hodgkin-Huxley model to implement ionic conductances realistically.

AMPA, NMDA and GABA receptors have also been modelled along with detailed Ca^{2+} dynamics. Hodgkin-Huxley channels [11] have been added and conductances, G_k and G_{Na} , are calculated

using:

$$G_{Na} = \bar{g}_{Na} \cdot m^3 \cdot h \quad (1)$$

$$G_k = \bar{g}_k \cdot n^4 \quad (2)$$

where m and h correspond respectively to the activation and inactivation variables of the sodium channels, n is the activation of the potassium channels and \bar{g} is the maximal channel conductance.

The NMDA receptor model used is a modified GENESIS-sim function “synchan”, which allows the user to create a synaptically activated channel to their own specifications. In the software, the modified synchan calculates the synaptic weight change in terms of post- and presynaptic activity. By altering this channel, we have created an NMDA receptor which updates the weight change of the AMPA synapses based on the NMDA receptor activation. Therefore by adding parameters which control the timing of the NMDA receptor activation, we can directly affect Ca^{2+} influx into the postsynapse.

The NMDA-R conductance depends on the cell membrane potential, V_m , as well as being dependent on Magnesium, which obstructs the NMDA-R until the cell becomes depolarised and allows the receptor to become permeable to Na^+ , K^+ and Ca^{2+} ions. The conductance is calculated using:

$$g_{NMDA}(t) = \bar{g} \frac{e^{-\frac{t}{\tau_1}} - e^{-\frac{t}{\tau_2}}}{1 + \eta[Mg^{2+}]e^{-\gamma V_m}} \quad (3)$$

with rise and decay times $\tau_1 = 2$ ms, $\tau_2 = 100$ ms and maximal conductance, \bar{g} . The Magnesium-block parameters are: $\gamma = 0.06/\text{mV}$, $\eta = 0.33/\text{mM}$ and magnesium concentration, $[Mg^{2+}] = 2\text{mM}$.

During biologically realistic circumstances when the NMDA receptor activates and opens, there is an influx of Ca^{2+} ions into the postsynaptic membrane allowing a change in plasticity to take place. This then triggers an *upregulation* of AMPA receptors to the postsynaptic membrane causing a long-lasting increase in the “Excitatory-Postsynaptic Potential”. EPSPs summate to depolarise the cell which in turn allows an increase in synaptic plasticity (LTP) through the increase of Ca^{2+} ions into the postsynaptic NMDA receptor. In the model we translate this as NMDA receptors calculating the change in synaptic plasticity through the use of a biophysical learning rule, then signalling these changes to the AMPA receptors which then physically implement the weight-change

as seen in Figure 2, below.

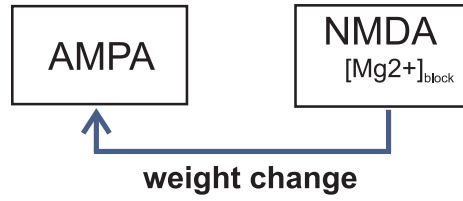


Figure 2: Block Diagram of how NMDA signals weight change from the learning rule. Na^+ ions enter the AMPA receptor allowing depolarisation of the cell membrane. This removes the Mg^{2+} block from the NMDA receptor and allows an influx of calcium through the receptor. The NMDA receptor acts as a “second messenger” calculating the weight change (implemented using a learning rule) and passing this to the AMPA receptor to update.

2.1 The Learning Rule

The main objective of the research to date was to come up with a single learning rule which allowed bidirectional plasticity changes to be modelled in a realistic manner. This meant that the rule used would have to encompass both presynaptic and postsynaptic cell mechanisms to be able to achieve this. To see how the rule is broken up into the separate elements which make up the intricate mechanisms undergone during LTP and LTD, we can refer to the block diagram shown in Fig. 3 and compare to learning rule below (Equation 4).

The learning rule updates the AMPA receptor weight, $\Delta\rho$, with every step of the simulation and is as follows:

$$\Delta\rho = LTP + LTD \quad (4)$$

where:

$$LTP = \mu \cdot NMDA_{act} \cdot \Theta([Ca^{2+}]'_i) \quad (5)$$

and:

$$LTD = \gamma \cdot NMDA_{act} \cdot \Theta(-[Ca^{2+}]'_{filt}) \quad (6)$$

$\Delta\rho$ is the continual update/change in AMPA weight at every simulation step. μ and γ are respective learning rates for LTP and LTD. $[Ca^{2+}]'_i$ is the derivative of the intracellular calcium concentration. $NMDA_{act}$ is the activation of the NMDA receptors that allow the influx of Ca^{2+} into the postsynaptic cell. Θ is the Heaviside function, representing the positive part of the derivative taken. $[Ca^{2+}]'_{filt}$ is the term which describes the negative derivative of the filtered intracellular calcium concentration and this filtering is done by a leaky integrator circuit.

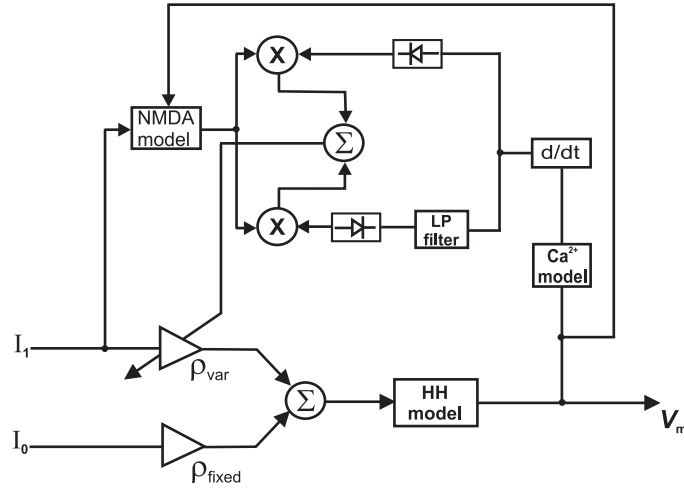


Figure 3: Block Diagram of STDP learning rule used. I_1 represents the variable spiking-event (current injection) timing, which can be altered to give either LTD or LTP depending on its occurrence before or after the fixed input, I_0 . These two inputs are summated to give the timing difference between post and presynaptic spiking, T . In both parts of the learning rule there are HH ion channels and detailed calcium dynamics modelled. For both LTP and LTD, the derivative of the calcium concentration, $[Ca^{2+}]'_i$ is found. For LTP, the positive derivative of the $[Ca^{2+}]_i$ is taken. For LTD, the derivative is put through a lowpass leaky-integrator filter before taking the negative derivative of this. Both the positive and negative derivatives are dependent on NMDA-receptor activation which will affect the change in plasticity.

2.2 LTD - The leaky integrator filter

As mentioned, $[Ca^{2+}]'_{filt}$ is the negative part of the derivative of the intracellular calcium concentration ($[Ca^{2+}]'_{filt} < 0$). Using a simple differential equation to give lowpass filtering of the calcium concentration, the derivative was calculated and then the negative part was used in the learning rule. The leaky integrator equation is in the form:

$$[Ca^{2+}]'_{filt} = [Ca^{2+}]'_{filt} + [Ca^{2+}]_i - ([Ca^{2+}]'_{filt} \cdot \tau) \quad (7)$$

$[Ca^{2+}]'_{filt}$ is the filtered calcium concentration and τ is the filter time constant. It was decided the leaky integrator was a suitable model for LTD after it was shown that LTD can be described by a mechanism which integrates postsynaptic Ca^{2+} signals [6]. It was shown that having a slow and steady decay in $[Ca^{2+}]_i$ would result in LTD as opposed to LTP which occurs when there is a transient increase in $[Ca^{2+}]_i$.

Comparing the calcium concentration (Fig. 4, solid line) to the lowpass filtered concentration (Fig. 4, dashed line) we can see a slower decay in the concentration.

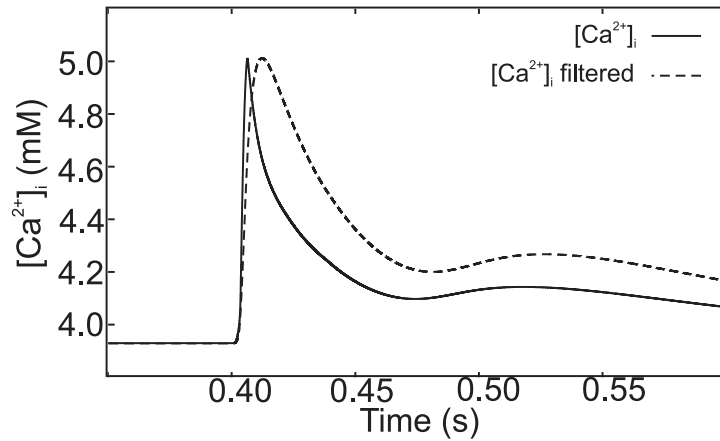


Figure 4: Comparison between $[Ca^{2+}]_i$ (solid line) and leaky-integrator filtered Ca^{2+} (dashed line). A slower, longer decay in the calcium concentration is achieved using the leaky integrator filtering. Filter constant $\tau = 0.8\text{ms}$

2.3 Calcium Dynamics

The calcium model used was of the form:

$$dCa^{2+}/dt = B \cdot I_k - Ca^{2+}/\tau \quad (8)$$

modelling a low threshold calcium current, $I_{Ca^{2+}}$, with parameters: $\bar{g}_{Ca^{2+}} = 1.75\text{mS}/\text{Cm}^2$, $\tau_{Ca^{2+}} = 30\text{ms}$, $[Ca^{2+}]_i = 2\text{mM}/\text{litre}$, $B = 1e12$. Ca^{2+} is the resulting concentration of the calcium ions and Ca_{base}^{2+} is the base-level concentration, giving $Ca^{2+} = Ca_{base}^{2+} + Ca^{2+}$.

The derivative of the $[Ca^{2+}]_i$ is split into its positive part, $\Theta([Ca^{2+}]'_i)$, and the negative derivative of the filtered intracellular calcium concentration, $\Theta(-[Ca^{2+}]'_{filt})$. The current injection, I_0 , occurs at 0.40s during the simulation and allows the NMDA-R magnesium block to be lifted, enabling a rise in the intracellular calcium concentration. Figure 5 shows how the postsynaptic Ca^{2+} mechanisms are split into the separate terms which determine whether LTP or LTD will occur.

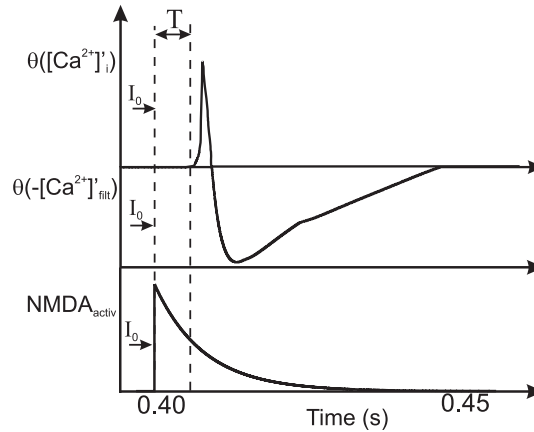


Figure 5: (a). Positive derivative of Ca^{2+} concentration, $[Ca^{2+}]'_i$, is used to model the positive part of the postsynaptic Ca^{2+} influx seen during LTP. (b). $[Ca^{2+}]'_{filt}$; the negative part of the filtered Ca^{2+} ($[Ca^{2+}]'_{filt} < 0$). We do this by filtering the calcium concentration using a leaky integrator model (Section 2.2), then taking the negative part of its derivative. (c). Activation of NMDA-R allows the influx of intracellular calcium to the postsynaptic receptor. Depending on how fully the receptor opens, the synaptic plasticity can either increase or decrease (LTP or LTD). I_0 , the current injection, results in depolarisation of the cell which in turn enables the postsynaptic NMDA-Rs to open. T is the delay between I_0 and the NMDA-R opening, thus, any influx of Ca^{2+} into the receptor is delayed by T .

3 Results

Each simulation ran through 150,000 steps and STDP curves were generated by running single simulations repeatedly with a time shift ‘ T ’ between pre- and postsynaptic spiking events, starting from $t = -0.10$ to $t = 0.10$ and shifting in increments of 0.001. The single simulation run-time is calculated by multiplying the number of simulation steps by $dt = 4e^{-6}$, giving a time of 0.6s.

3.1 Pyramidal cell, no interneuron

In Figure 6, we have plotted three STDP curves, each using a different ‘ τ ’ value ($\tau = 0.8$ ms, 0.05 ms and 5 ms) for the filtering of the Ca^{2+} outflux. On the Y-axis we have the change in weight, $\Delta\rho$, and this is plotted against the interspike interval T (X-axis) which is the timing between pre- and postsynaptic spiking. The interspike interval is calculated by finding the values of the time of presynaptic spiking, t_{pre} , and subtracting this from the postsynaptic timing, t_{post} . It is observed that different filtering of the $[Ca^{2+}]_i$ produces three noticeably different STDP curves. While the LTP part remains consistently the same, we can clearly see there are three distinct alterations seen in the LTD part of the curve. By changing the decay constant ‘ τ ’ of the leaky integrator, we can directly affect the shape of the LTD seen which in turn changes the STDP plot shapes. Comparing Fig. 6(a) to Fig. 6(b), it can be observed that the time LTD is present during the negative time window is much longer. When the filter has a short decay time (Fig. 6(c)), there is a noticeable decrease in time as well as magnitude of LTD present. We can also make the general observation that the STDP curve Fig. 6(a) is strikingly similar to results seen in vitro [1, 2, 3].

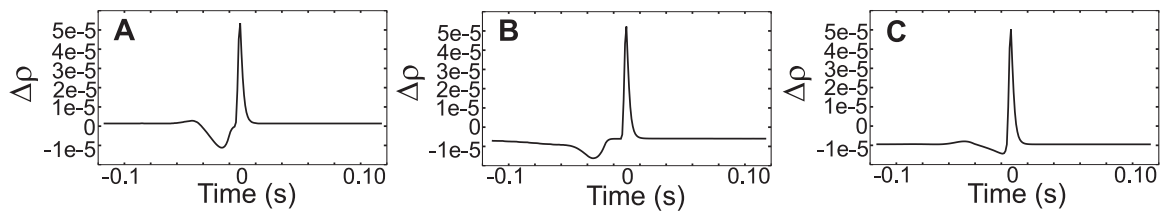


Figure 6: STDP using leaky-integrator modelled LTD. (a). Leaky integrator time constant, $\tau = 0.8$ ms. STDP curve looks like the expected asymmetrical weight-change curve. (b). Filtering of $[Ca^{2+}]_i$ with $\tau = 0.05$ ms now gives a longer and larger LTD part to the STDP curve. (c). When the decay constant is set to $\tau = 5$ ms, LTD significantly diminishes and lasts only for a short period.

3.2 Pyramidal cell with attached interneuron

As mentioned in Figure 1, the attached interneuron is a modelled GABAergic chandelier cell with NMDA and GABA receptors, along with detailed HH channels [11].

However, instead of plotting three different curves using the different ‘ τ ’ values, we have chosen the ‘ τ ’ (0.8 ms) which allows for the most biologically accurate output. Again the weight change, $\Delta\rho$, is plotted against the interspike interval, T . When looking at the STDP curve of pyramidal cell with attached interneuron (solid lines) in comparison to without interneuron (dashed lines) in Fig. 7, it is interesting to observe the decline in magnitude and shape of LTD, while long-term potentiation remains the same. This is due to the dual nature of the GABAergic interneuron. It was found by Aihara [5] and also explained by Edward O’ Mann [12] that fast spiking GABAergic interneurons cause a phenomenon known as “shunting inhibition” on the pyramidal cell [12]. GABA receptors are connected to chloride channels (Cl^-) which have a reversal potential near to that of the resting membrane potential of the pyramidal cell ($E_{\text{Cl}^-} = E_{\text{rest}} = -65\text{mV}$). When the Cl^- channels are activated they cause small, brief, but significant changes to the membrane potential, V_m which result in large increases in conductances. This is the process of shunting inhibition. Doiron et al [13] show that during subthreshold frequencies (10Hz - 15Hz), shunting gain control acts divisive in nature. That is, the GABAergic effects of the interneuron division operation can be seen directly in Figure. 7 as diminished magnitude and shaping of the LTD part of the STDP curve.

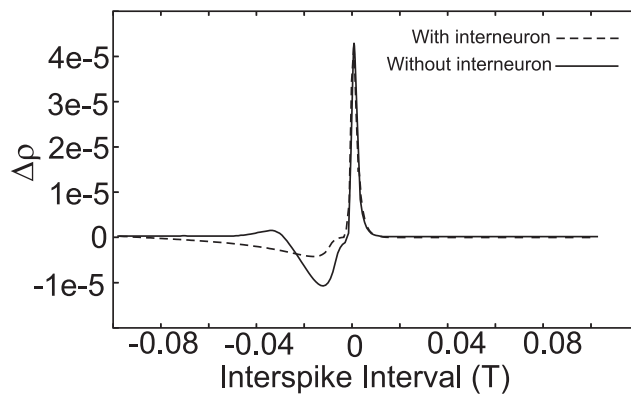


Figure 7: Comparison between STDP plots of pyramidal cell with (dashed line) and without (solid line) interneuron, both using $\tau = 0.8$ ms. By comparing the STDP curve with attached interneuron to without interneuron (dashed line), a distinct decrease in magnitude in LTD is seen, which causes a noticeable shape change to the curve.

3.3 Reducing the NMDA activation: Further applications

NMDARs are responsible for the majority of calcium influx into a cell [14]. Therefore if there is an impairment to the NMDA receptors, we should observe two effects; a distinct decrease in magnitude of plasticity and a reduction in inhibition from the attached interneuron. From this, we can predict that a sizeable reduction in magnitude of the overall STDP curve should be seen as well as a complete change in shape to what was observed in Fig. 10. When we study the effects the attached interneuron and NMDA receptor impairment has on the STDP curve, it is reasonable to conclude that reducing NMDA-R activity impairs the GABAergic inhibition on the pyramidal cell by decreasing the GABAergic conductance, \bar{g}_{GABA} . This disinhibition of the pyramidal cell's excitatory activity (due to the reduced GABA conductance \bar{g}_{GABA}) allows the pyramidal cell's membrane potential to increase, causing a potentiation in synapse strength during the negative timing window. Therefore, the amount of LTD seen in comparison to that seen in Fig. 8 is less.

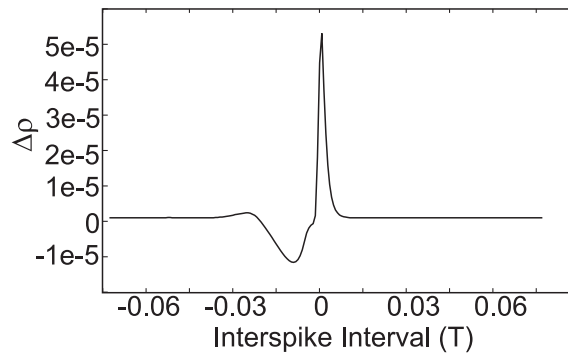


Figure 8: Reducing the NMDA receptor activity affects both the pyramidal cell and interneuron. Reduced NMDA activity will cause a decline in the influx of intracellular calcium into the pyramidal cell. Thus, any plasticity changes seen during LTP and LTD will be proportionally smaller and in ratio to the NMDA receptor activity. In addition to this, reduction in NMDA receptor activity will also affect the GABAergic interneuron. The reduction in NMDA-R activity means that the interneuron's ability to produce inhibitory GABAergic neurotransmitters will be drastically impaired. In turn, this causes the reduction in LTD previously seen in Fig. 10 to be markedly reversed.

4 Discussion and Next Steps

We have shown that it is possible to model Ca^{2+} dependent LTD realistically during STDP simulations. Rather than have set Ca^{2+} thresholds which determine whether LTP or LTD should take place, as is the case with Shouval's model [15], our approach focuses on using the positive and negative $[\text{Ca}^{2+}]_i$ derivatives to model both LTP and LTD. By using our biophysically realistic learning rule, which applies differential Hebbian learning to scale the LTP/LTD parts separately, we have eliminated the positive-timing LTD that was seen by Shouval and Aihara [5, 15], but *not* seen during in-vitro experiments [1, 2, 3]. Our model eliminates positive-timing LTD through the slow release of calcium, meaning the IPSPs generated during the LTP-window will not be strong enough to cause depolarisation of the postsynaptic membrane, thus eliminating the decline in synaptic strength.

Comparing our new learning rule to those such as the ISO learning rule [7, 8, 9, 10], the greatest noticeable difference between the two is the inclusion of Hodgkin-Huxley parameters and realistic calcium dynamics. Also, it can be noted that our new learning rule has been split into two separate terms which describe the pre- and postsynaptic mechanisms of LTP and LTD rather than one term describing all. This allows for a greater precision in the modelling of the cellular processes undergone during spike-timing plasticity.

In our implementation of the leaky integrator filtering of Ca^{2+} , we have shown that it is possible to model the relationship between Ca^{2+} dynamics and LTD, as stated by Tanaka [6]. This implies that the leaky integrator mechanism could realistically be a postsynaptic cell mechanism responsible for LTD.

We know that hypofrontality is a condition seen in patients with schizophrenia, and with our model we have replicated this decrease in cortical activity. By reducing the NMDA receptor activity, we are actively causing an increase in the LTD seen, shifting the ratio of LTD/LTP towards that of LTD. Observing our results when NMDA-R activation is reduced (Fig. 8), the inhibition that was seen when attaching an interneuron (Fig. 10) has now been reversed and causes an *increase* in LTD. Using this information along with studying the effects of NMDA-R impairment on the inhibitory interneuron, we can note the obvious changes in the balance between LTP and LTD. It was seen by Tegner et al and Song et al that the ratio of LTD to LTP ($\alpha = \text{LTD}/\text{LTP}$) is essential for

stable learning to occur [16, 17]. In particular, a balanced firing rate requires a learning ratio slightly larger than unity. ($\alpha = \text{LTD}/\text{LTP} > 1.00$). We hypothesise that the NMDA-R reduction causes a shift in the balance between LTD/LTP causing the alpha value, α , to become significantly larger than unity gain. We propose the larger ratio of LTD to LTP acts as a catalyst in causing hypofrontality. Expanding our model to a larger network would allow observations in the change in ratio of depression to potentiation, $\alpha = \text{LTD}/\text{LTP}$, towards LTD in patients with hypofrontality.

Thus, a possible application for this model would be to develop the microcircuit into a larger network of neurons and observe working memory when there is NMDA receptor impairment. This type of model would be of interest to those who are working in the research field of schizophrenia [18, 19].

References

- [1] H. Markram, J. Lübke, M. Frotscher, and B. Sakman. Regulation of synaptic efficacy by coincidence of postsynaptic APs and EPSPs. *Science*, 275:213–215, 1997.
- [2] J. C. Magee and D. Johnston. A synaptically controlled, associative signal for Hebbian plasticity in hippocampal neurons. *Science*, 275:209–213, 1997.
- [3] Guo-qiang Bi and Mu-ming Poo. Synaptic modifications in cultured hippocampal neurons: Dependence on spike timing, synaptic strength, and postsynaptic cell type. *J. Neurosci.*, 18(24):10464–10472, 1998.
- [4] D. O. Hebb. *The organization of behavior: A neuropsychological theory*. Wiley-Interscience, New York, 1949.
- [5] T. Aihara, Y. Yamazaki, Y. Abiru, Y. Fukushima, H. Watanabe, and M. Tsukada. The relation between spike-timing dependent plasticity and Ca^{2+} dynamics in the hippocampal CA1 network. *Neuroscience*, 145:80–87, 2007.
- [6] K. Tanaka, L. Khiroug, F. Santamaria, T. Doi, H. Ogasawara, G. C. R. Ellis-Davies, M. Kawato, and G. J. Augustine. Ca^{2+} requirements for cerebellar long-term synaptic depression: Role for a postsynaptic leaky integrator. *Neuron*, 54:787–800, June 2007.
- [7] A. Saudargiene, B. Porr, and F. Wörgötter. How the shape of pre- and postsynaptic signals can influence STDP: A biophysical model. *Neural Comp.*, 16:595–626, 2004.
- [8] B. Porr and F. Wörgötter. Learning with “relevance”: Using a third factor to stabilise hebbian learning. *Neural Computation*, 19:2694–2719, 2007.
- [9] B. Porr and F. Wörgötter. Isotropic Sequence Order learning. *Neural Comp.*, 15:831–864, 2003.
- [10] B. Porr and F. Wörgötter. Isotropic sequence order learning using a novel linear algorithm in a closed loop behavioural system. *Biosystems*, 67(1–3):195–202, 2002.
- [11] A.L.Hodgkin and A.F.Huxley. A quantitative description of membrane current and its application to conduction and excitation in nerve. *J.Physiol*, 17(4):500–544, 1952.

- [12] E. O'Mann and O. Paulsen. Keeping Inhibition Timely. *Neuron*, 49(1):8–9, 2006.
- [13] B. Doiron, N. Berman A. Longtin, and L. Maler. Subtractive and Divisive Inhibition: Effect of Voltage-Dependent Inhibitory Conductances and Noise. *Neural Computation*, 13:227–248, 2000.
- [14] T. G. Oerthner B. L. Sabatini and K. Svoboda. The life cycle of Ca^{2+} ions in dendritic spines. *Neuron*, 33:439–452, 2002.
- [15] M. F. Bear H. Z. Shouval and L. N. Cooper. A unified model of NMDA receptor-dependent bidirectional synaptic plasticity. *PNAS*, 99(16):10831–10836, August 2002.
- [16] K. D. Miller S. Song and L.F. Abbott. Competitive hebbian learning through spike-timing-dependent synaptic plasticity. *Nature Neurosci*, 3:919–926, 2000.
- [17] J. Tegnér and A. Kepecs. Why neuronal dynamics should control synaptic learning rules. in: Dietterich tg; becker s; ghahramani z (eds). *Adv Neural Inf Process Syst*, 14, 2002. MIT Press, Cambridge, MA.
- [18] B. J. Morris, S. M. Cochran, and J. A. Pratt. PCP: from pharmacology to modelling schizophrenia. *Current opinion in Pharmacology*, 5, 2005.
- [19] D. Rujescu, M. Keck A. Bender, F. Ohl A.M. Hartmann, I. Giegling H. Raeder, H. Moller J. Genius, R. W. McCarley, and H. Grunze. A pharmacological model for psychosis based on N-methyl-D-aspartate Receptor hypofunction: Molecular, Cellular, Function and Behavioral abnormalities. *Biological Psychiatry*, 59(8):721–729, 2006.

Appendix

A Abbreviations

$[Ca^{2+}]_i$: Intracellular calcium concentration

Ca^{2+} : Calcium ion

Cl^- : Chloride ion

K^+ : Potassium ion

Mg^{2+} : Magnesium ion

Na^+ : Sodium ion

AMPA: α -amino-3-hydroxy-5-methyl-4-isoxazolepropionic acid

GABA: γ -amino-butyric-acid

NMDA: N-methyl-D-aspartic acid

EPSP: Excitatory Postsynaptic Potential

IPSP: Inhibitory Postsynaptic Potential

ISO: Isotropic Sequence Order (Learning) [7, 8, 9, 10]

LTD: Long term depression

LTP: Long term potentiation

STDP: Spike-timing-dependent plasticity

B GENESIS Compartmental equation

The differential equation representing each compartment solved by GENESIS is as follows:

$$C_m \frac{dV_m}{dt} = \frac{(E_m - V_m)}{R_m} + \sum_k [(E_k - V_m)G_k] + \frac{(V'_m - V_m)}{R'_a} + \frac{(V''_m - V_m)}{R''_a} + I_{inject} \quad (9)$$

V_m represents the membrane potential at a point inside the compartment, relative to the “ground” outside the cell. The membrane capacitance C_m can be charged or discharged as current flows into or out of the compartment and thus changing the value of V_m . This current can come from adjacent compartments, from ions passing through ion channels, or from a current “ I_{inject} ” injected into the

compartment via a probe. The “leakage resistance”, R_m , and the related equilibrium potential E_m represent passive channels in the cell. G_k represents the variable conductance specific to individual and combinations of ions. Each of the conductances have an associated equilibrium potential, E_k . The equilibrium potential, or “Reversal Potential” is the value of V_m for when the net flow of ions through the conductance equals zero. In GENESIS, these conductances are calculated from the Nernst Equation. “ k ” is used to represent any of the various types of conductances (Na^+ , K^+ , Cl^- , etc) modelled in the compartments.

C Hodgkin-Huxley calculations in GENESIS

Hodgkin and Huxley’s work in 1952 [11] broke down the ionic processes taking place during the depolarisation of a cell membrane. They showed that when there is an increase in the cell’s membrane potential, V_m , sodium channels open and Na^+ ions flow into the cell. The influx of the Na^+ ions cause the Na channel conductance to increase which then results in an action potential being fired. The action potential occurs when the increase in membrane potential reaches a threshold value of ≈ -45 mV. After some time, the sodium channels become inactivated and the potassium channels open, which causes a flow of charge back out the cell with the efflux of the K^+ ions, ending the action potential.

The Hodgkin-Huxley conductances as stated previously in Equations (1) and (2) are:

$$G_{Na} = \bar{g}_{Na} \cdot m^3 \cdot h$$

and

$$G_k = \bar{g}_k \cdot n^4$$

Where n is the activation of the potassium channel. The sodium channel conductance, G_{Na} , is calculated from the product of the activation variable m and the inactivation variable h . This conductance decreases as the membrane potential V_m increases.

The activation and inactivation parameters are solved in GENESIS using:

$$\frac{dn}{dt} = \alpha(V)(1 - n) - \beta_n(V)n$$

$\alpha(V)$ and β_n are voltage-dependent “rate” parameters. They are both related to the steady state value of the activation parameter, n_∞ , and the time to reach this value, τ_n , through the equations:

$$\alpha_n(V) = \frac{n_\infty(V)}{\tau_n(V)}$$

and

$$\beta_n(V) = \frac{1 - n_\infty(V)}{\tau_n(V)}$$

D The Nernst Equation

The Nernst equation is used to calculate the equilibrium voltage potential for an ion:

$$E_{ion} = 2.303 \frac{RT}{zF} \log_{10} \frac{[ion]_o}{[ion]_i}$$

E_{ion} is the ionic equilibrium potential, or “resting potential”, R is the universal gas constant, T is absolute temperature (and proportional to E_{ion}), z is the charge of the ion, and is inversely proportional to E_{ion} . F is Faraday’s constant and $[ion]_i$ and $[ion]_o$ are the ionic concentrations inside and outside the cell, respectively.

These are simplified when calculating at body temperature (37°C) as $\frac{RT}{F}$ becomes a constant:

$$E_k = 61.54mV \cdot \log_{10} \frac{[K^+]_o}{[K^+]_i}$$

$$E_{Na} = 61.54mV \cdot \log_{10} \frac{[Na^+]_o}{[Na^+]_i}$$

$$E_{Ca} = 30.77mV \cdot \log_{10} \frac{[Ca^{2+}]_o}{[Ca^{2+}]_i}$$

Thus, when calculating the membrane resting potential at body temperature, we only need to know the intracellular and extracellular concentrations of the specific ions we are interested in.

E Gantt chart of six month schedule

Detailed Plan for next six months						
Task	May 2008	June 2008	July 2008	Aug. 2008	Sept. 2008	Oct. 2008
Write/Submit Papers with current results	■					
Begin Mathematical Model of circuit		■				
Present work as poster presentation in Geneva			■			
Expand microcircuit into network of neurons				■		
Meet with Neuroscientists to hopefully endorse collaboration using network model				■		
Submit work with mathematical proof to Neural Computing journal				■		
Present results at conference					■	
Discuss further applications of model					■	

Figure 9: Gantt chart overviewing schedule for next six months

F Gantt chart for rest of project

Timetable for rest of PhD work (months)														
Task	Nov 2008	Dec 2008	Jan 2009	Feb 2009	Mar 2009	Apr 2009	May 2009	June 2009	July 2009	Aug 2009	Sept 2009	Oct 2009	Nov 2009	Dec 2009
Alter model based on feedback	█													
Present Results to date		█												
Conclude experiments					█									
Analyse and Present Results						█	█	█						
Thesis Abstract							█							
Thesis								█						

Figure 10: Gantt chart outlining schedule for rest of project